Experimental Thermal and Fluid Science 32 (2008) 1504–1511

Contents lists available at ScienceDirect

Experimental Thermal and Fluid Science

journal homepage: www.elsevier.com/locate/etfs

Experimental analysis of bubble growth, departure and interactions during pool boiling on artificial nucleation sites

S. Siedel, S. Cioulachtjian, J. Bonjour *

CETHIL – UMR5008 CNRS INSA-Lyon Univ. Lyon1, Bât. Sadi Carnot, 9 rue de la Physique, INSA-Lyon, F-69621 Villeurbanne Cedex, France

ARTICLE INFO

Article history:
Received 23 December 2007
Received in revised form 9 April 2008
Accepted 10 April 2008

Keywords:
Pool boiling
Bubble growth
Bubble coalescence

ABSTRACT

The present work describes experimental results of pentane pool boiling, simplified to the cases of boiling on a single or on two adjacent nucleation sites. Bubbles growths have been recorded by a high speed camera under various wall superheat conditions. Bubble volume has been plotted as a function of time, and an experimental growth law has been proposed. Oscillations were observed during growth, showing the interaction of one bubble with the preceding bubble released from the same nucleation site. Lateral coalescence has been visualized and the images have brought to the fore the capillary effects on the distortion of the interface.

1. Introduction

Boiling has received much attention for decades because of the many technological applications in which this phenomenon is involved. It still remains as one of the major research topics because of the high number and the variety of scales of the physical mechanisms involved. Modelling boiling requires many hypotheses whose validity can not always be assessed. This results in a large number of different models, often with corrective factors. The results predicted by these models are sometimes far from the experimental results. Experiments in boiling also receive their share of difficulties. Phenomena are fast, bubbles interact, scales are multiple, material properties are not always well defined, especially the wall roughness, and physical parameters are hard to measure in fluids. Boiling needs to be simplified in order to identify the role of the different mechanisms involved.

Among the recent works on single bubble nucleate boiling, Golobic et al. [1] determined experimentally the transient wall temperature distributions under growing bubbles on a thin heated foil. They found that the temperature distribution under the bubble is first a peaked-distribution, and then shifts to a crater-distribution. Moreover, they did not observed any large thermal influence area around the bubble. Cheng and Burkhardt [2] suggested a method for bubble identification and tracking when recording boiling. This method allows studying single bubbles while boiling on a natural surface. Van der Geld [3] theoretically predicted the dynamic contact angle of a truncated spherical bubble growing on a heated surface. This angle can lead to the determination of the detachment volume. Di Marco et al. [4] experimentally measured the rising velocity of bubble after detachment, showing gaps in the available models, and Vasquez et al. [5] compared three measurement techniques for the determination of the bubble size at detachment.

Several analytical models describing bubble growth have been developed during the last decades. Among the first models was the theory of Bosnjakovic and Jakob, which is explained by Zuber [6]. The bubble was assumed to be spherical and at saturation temperature in a homogeneous superheated liquid. The heat transfer was driven by conduction through the thermal boundary layer, resulting to a bubble growth model giving $R_{eq} \propto t^{0.5}$. The 0.5 exponent was obtained by integration of the transient conduction equation in the boundary layer. Many authors developed other models since then. They successively complicated the system description or the assumptions, and gave more or less weight to the different heat transfer mechanisms involved. Plesset and Zwick [7] considered the bubble as a sphere tangent to a wall in a homogeneous superheated liquid, with a thin thermal boundary layer around the bubble. Scriven [8] had a similar model including convective heat diffusion in the liquid instead of assuming a thin boundary layer. He therefore needed to assume a growth law $R_{eq} = C \times t^{0.5}$ and looked for the C coefficient. Mikic et al. [9] also used a uniform temperature field from the superheated wall to a saturated bulk liquid. They also assumed the bubbles to be spherical and tangent to the wall. Cooper and Lloyd [10] considered the existence of a liquid microlayer beneath the bubble. Most of the heat transferred to the bubble was conducted through this microlayer. The bubble was hemi-spherical on a wall, in a temperature field. The bubble was assumed to be large compared to the thermal boundary layer. The bulk liquid was at saturation temperature or slightly

* Corresponding author. Tel.: +33 4 72 43 64 27; fax: +33 4 72 43 88 11.
E-mail address: jocelyn.bonjour@insa-lyon.fr (J. Bonjour).

0894-1777/$ - see front matter © 2008 Elsevier Inc. All rights reserved.
doi:10.1016/j.expthermflusci.2008.04.004

Nomenclature

A	ratio of the height of the gravity centre to the equivalent radius: $A = h_{cg}/R_{eq}$
h_{cg}	height of the centre of gravity (m)
P	pressure (Pa)
R_1, R_2	main curvature radii of an interface (m)
R_{eq}	equivalent radius of a bubble (m)
T	temperature (K)
T_{sat}	saturation temperature (K)
t_{wall}	wall temperature (K)
t	time (s)
t_d	bubble growth time (s)
t'	non-dimensional time: $t' = t/t_d$
V	volume (m^3)
V_d	bubble departure volume (m^3)
V'	non-dimensional volume: $V' = V/V_d$

subcooled. Due to their formulation, all these different theoretical studies lead to a growth law as $R_{eq} \propto t^{0.5}$.

More recent works used numerical simulation to allow the resolution of less simplified and more tightly coupled equations systems. One of the last models was developed by Das et al. [11]. It is still assumed that there is no interaction between successive or adjacent bubbles, and that the generation of single bubbles from each nucleation site is not influenced by the surroundings. This assumption cannot be sustained in our single bubble experiments. The waiting time between two successive bubbles was very short, so that even at low wall superheat, a new bubble was generated in the nucleation site while the previous bubble was still close to the wall.

Bubble growth rate has also recently been studied in the case of the presence of a surfactant by Hetsroni et al. [12]. They did not find any change on the bubble growth dynamics at low heat flux, but an increased detachment volume and a shorter life-time at high heat flux were described. Bubble growth was observed on an impulsively powered microheater by Yin et al. [13]. They found that the bubble growth consists of two steps, the first is a relatively violent one followed by shrinking of the vapour mass, and the second one is a slower expansion.

A few experiments have been performed to study the interaction and the coalescence of neighbouring bubbles. Bonjour et al. [14] suggested a map of nucleation site interactions, which allowed determining the site activation and bubble coalescence conditions with respect to the parameters of an experiment with 3 nucleation sites. Mukherjee and Dhir [15] experimentally and numerically studied lateral merger of vapour bubbles. They found that merger of multiple bubbles significantly increases the overall wall heat transfer, because of a liquid layer trapped between the bubble bases and of cooler liquid drown towards the wall during contraction after merger. Zhang and Shoji [16] studied the influence of the ratio of the nucleation site distance on the bubble departure diameter. They suggest three interaction mechanisms: coalescence, hydrodynamic bubble interaction and thermal nucleation site interactions. They established four different regions where the relative weight of each mechanism is different.

This brief introduction shows that much work remains to be done as regards bubble growth during boiling, and also that the interaction between bubbles during their growth is usually not well considered. The present study is focused on the growth and detachment of bubbles from a single nucleation site, and on the interaction between two bubbles growing on adjacent nucleation sites on a superheat wall in a saturated liquid. Shape and size of bubbles are recorded with a high speed camera, and computed by an automatic processing of the images. Wall and saturated liquid temperature are measured, and the heat flux transmitted to the fluid is computed.

2. Experimental apparatus and procedure

The experimental apparatus is made of an airtight aluminium parallelepiped tank ($250 \times 250 \times 180\ mm^3$). The tank has been depressurised to less than 1 mbar (absolute pressure) during 12 h, then filled with 99% purity *n*-pentane (Fig. 1). After filling the tank with pentane, the fluid has been heated to a temperature corresponding to a pressure higher than the atmospheric pressure, and several degassing of the liquid have been performed to ensure the absence of dissolved air. Three faces of the tank are equipped with windows allowing the observation of the boiling process. The chosen fluid, *n*-pentane, is not toxic, and allows to work with comfortable temperature and pressure conditions ($T_{sat} = 35.7\ °C$ at $P = 1$ bar). A heating element is used to warm up the pentane bath and to keep it at the chosen saturation conditions. Four thermocouples inside the tank allow to measure the temperatures in both liquid and vapour phases and to check their uniformity. The temperature in all experiments was homogeneous and the same in both phases.

The experimental sample, shown in Fig. 1, is made of a 20 mm diameter copper cylinder, heated by a 100 W cartridge heater. The heat flux is conducted through a 5 mm copper pin, equipped with six K-type thermocouples. On the top of the pin is soldered a 40 μm thin and 18 mm diameter copper plate. The plate is polished to avoid nucleation on its surface, and its thinness results in a radial temperature drop around the pin preventing nucleation on the edges of the plate. The whole experimental sample is insulated with Teflon®. The 6 thermocouples give the temperature profile in the pin, and a 2D conduction model allows calculating the surface temperature and the heat flux transmitted to the pentane. The surface temperature is known to be non-homogeneous and to vary with time because of the local heat flux variations under the bubble. However, the thermal diffusivity of copper is very high (about $1.1 \times 10^{-4}\ m^2/s$), the bubble size is small (about 1 mm diameter at departure) compared to the size of the copper pin (5 mm diameter), and the ratio of heat flux transmitted to the bubble is very low (less than 1% of heat flux is latent heat transfer, as measured in our experiments and [17]). Therefore, the temperature variation and non-homogeneity was minimized in these experiments. Thus, the wall temperature is assumed to be constant and homogeneous and will be used as a reference to analyse the results.

An artificial nucleation site is made by mechanical indentation at the centre of the plate. The site has been visualized with a confocal white light microscope (Fig. 2). It is paraboloidic, 500 μm deep and has a diameter of 180 μm. For bubble interaction experiments, a second identical site is made with a distance of 660 μm between the centres of the sites.

Bubbles are visualized and recorded laterally by a high speed camera (Photron Fastcam 1024 PCI). The typical image acquisition frequency was 3000 fps for single bubble experiments and 27,000 fps for lateral coalescence experiments. The image resolution is about 17×17 μm per pixel due to the optical magnifying system. A trade off for the aperture was sought: closing the diaphragm leads to a short depth of field (which is desirable), but limits the image brightness (which is not desirable). A short depth of field is required for a proper bubble contour detection at the nucleation site centre plane, and to avoid any interference

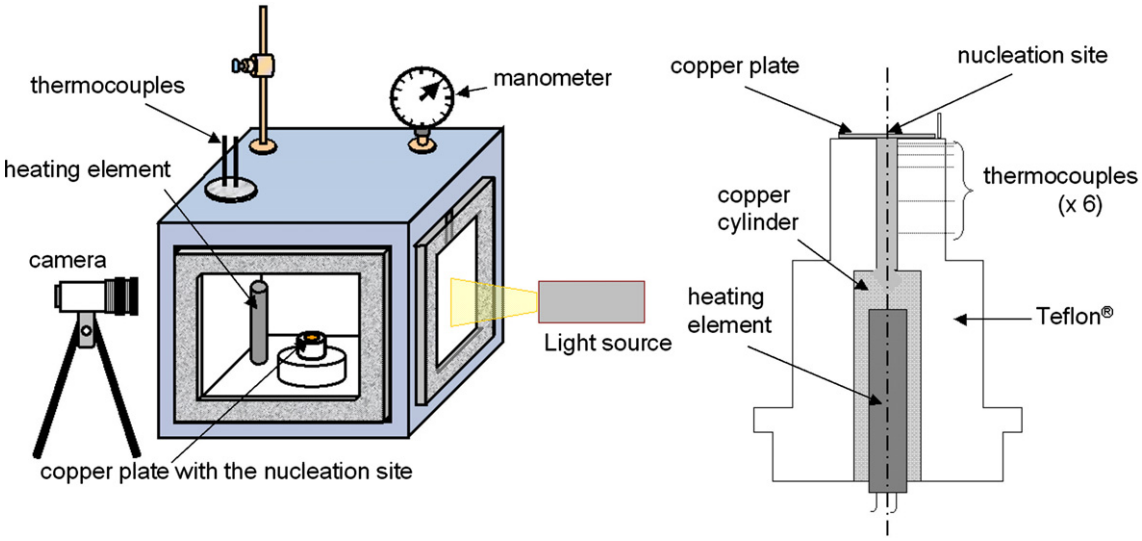

Fig. 1. Schematic of the experimental apparatus and test sample.

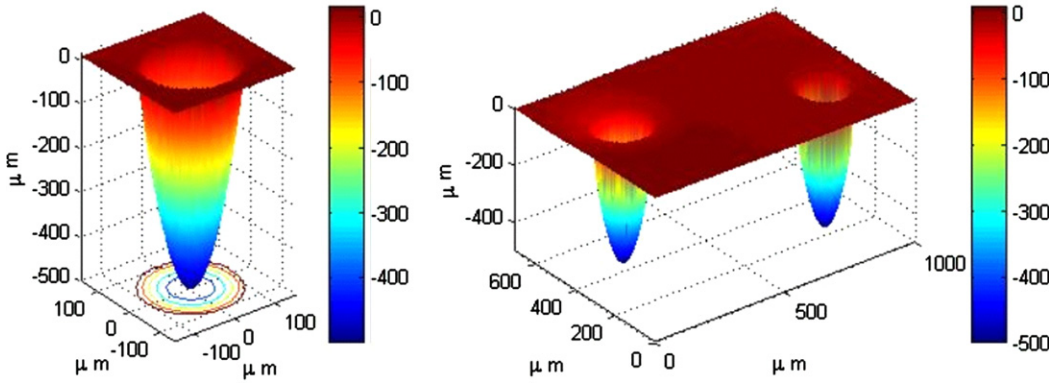

Fig. 2. Nucleation sites geometry obtained by means of confocal microscope observation.

of the background on the image processing. An image automatic processing software has been developed, allowing to determine the volume of the bubble, the height of its centre of gravity and the area of the interface for each image. Bubble contour is first determined by locating maximum grey gradient using Sobel method. The bubble's volume is measured as if the bubble was a stack of 17 μm thick (i.e., 1 pixel) vapour cylinders. To evaluate the height of the centre of gravity, the vapour pressure is supposed to be homogeneous inside the bubble, with low evolutions of pressure and vapour density in the bubble.

3. Results and discussion

The vapour volume has been calculated from the image processing. Other studies often use the equivalent diameter R_{eq}, i.e., the diameter of a sphere of equal volume, as the physical parameter to study bubble growth, because the growth models are based on a spherical or truncated spherical shape. The bubbles obtained in our experiments are not spherical (see Fig. 3), especially close to the moment of detachment. Therefore, the volume is chosen as the main parameter, since it is directly linked to mass transfer, i.e., to the latent heat transfer.

Bubble growth has been computed for different wall superheats (Fig. 4). The studied superheat range is limited by the deactivation of the nucleation site for low temperatures and by the occurrence of vertical coalescence for high temperatures. The bubble growth is reproducible, since the mean deviation of the bubble growth time is less than 6% and the mean deviation of the departure volume is less than 2% for different experiments performed with the same wall superheat. The bubble growth time is significantly reduced when increasing the wall superheat, whereas the departure volume remains almost unchanged (variations lower than 10%). The force balance that governs bubble departure does not seem to be much affected by the wall superheat, unlike the vapour production rate.

The bubble dynamics has then been compared for different superheats (Fig. 5). For a meaningful comparison, the growth curves have been normalized by dividing the time by the total growth time ($t' = t/t_d$), and the volume by the departure volume ($V' = V/V_d$). A very good similarity between the different curves is observed. Bubble growth, in all the conditions of the experiments can thus be described by a non-dimensional law that holds true for any wall superheat, as long as no bubble merging occurs.

The empiric law resulting from our experiments is $V' = t'^{0.6}$ for the bubble growth. However, for $t' < 0.2$, a better description is reached by $V' = 2t'$ (Fig. 5). These results are relatively consistent to those obtain by Lee et al. [18]. We must add here that bubble dynamics can be described independently from the wall superheat with that empiric law. Until now, most analytical analyses [6–11]

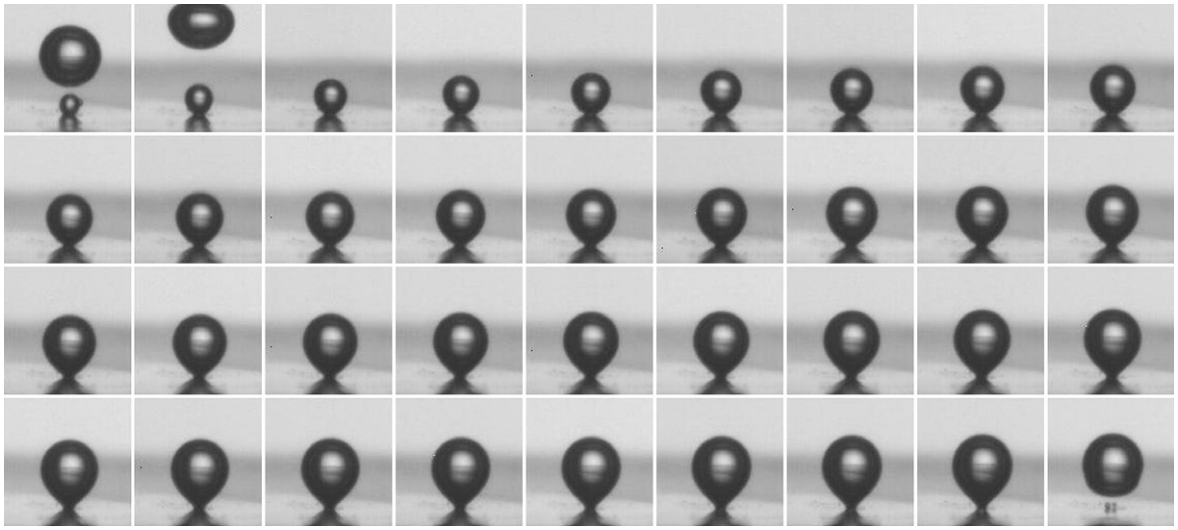

Fig. 3. Single bubble growth (375 fps, i.e., 1 image out of 8 at a video recording speed of 3000 fps).

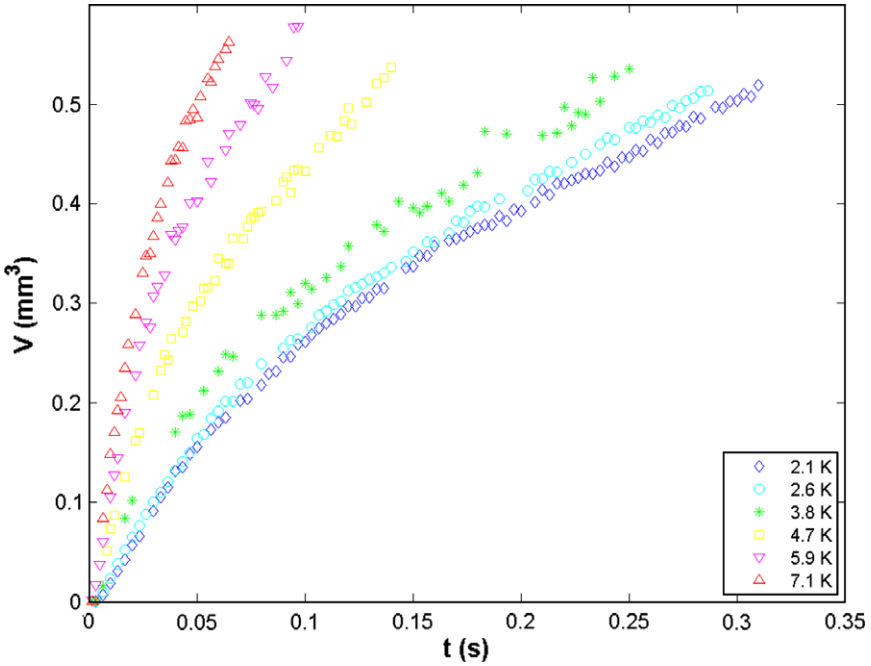

Fig. 4. Bubble growth dynamics at various wall superheats.

yield a power law as $R_{eq} \propto t^{0.5}$, i.e., $V' = t'^{1.5}$, for the thermal growth of a bubble. It must hence be underlined that the results of these analytical analyses are very different from our observations, because the models are highly simplified, owing to the complexity and the high number of physical mechanisms involved. The curvature of the bubble growth curve $V' = t'^{j}$ is even opposite in the models ($j > 1$) and to the experiments ($0 < j < 1$). All these observations lead to the conclusion that a better description of bubble growth is needed in order to model this phenomenon. Interactions with the previous bubble must be taken into account when modeling bubble growth. Hence, the initial conditions cannot be chosen with a still, well-establish thermal boundary layer in the case of two very near successive bubbles.

The volume generation rate has been computed by differentiating a high order polynomial best fit of the experimental data with respect to time (Fig. 6). This graph shows that even if the interface overall area increases, the vapour generation, i.e., the latent heat transfer, is decreasing with time. A possible interpretation is proposed: this observation may be attributed to the following mechanisms. First, the phase change mainly takes place close to the wall, where the liquid superheat is high. But when a bubble rises in the liquid after its detachment, it may draw up some liquid, so that the superheated liquid initially located around the bubble moves towards the nucleation site, resulting in an increase of the mass transfer during the beginning of the next bubble growth. Afterwards, the vapour production cools down the liquid around the new bubble, resulting in a drop of the vapour production rate.

Fig. 7 shows the ratio of the height of the centre of gravity to the equivalent radius of the bubble ($A = h_{cg}/R_{eq}$). The parameter '**A**' describes well the shape of a bubble. If the bubble is a sphere, **A** = 1. If it is a truncated sphere, **A** < 1. Furthermore, the oscillations are also described by this parameter. For high wall superheat, the curves

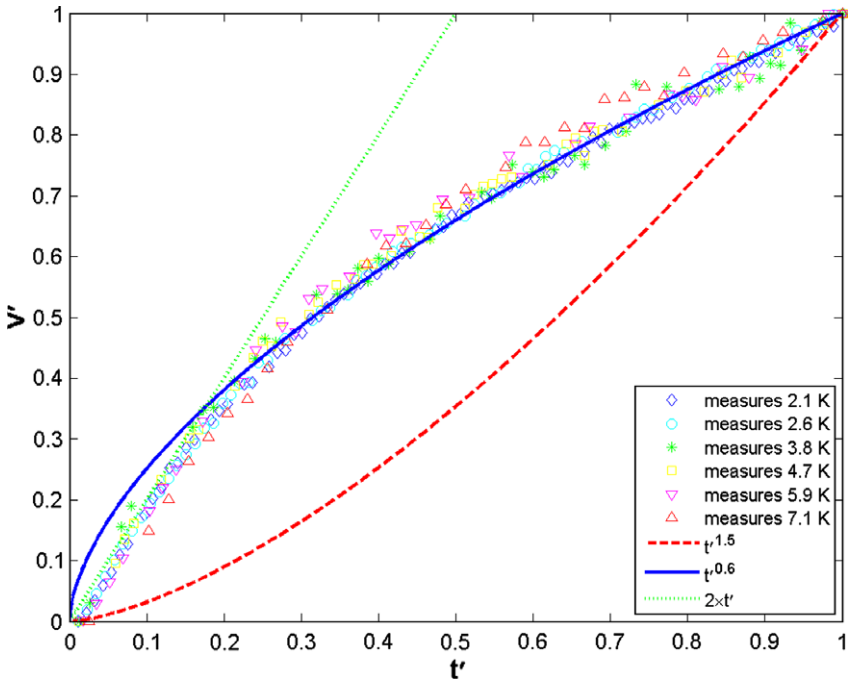

Fig. 5. Non-dimensional bubble growth at various wall superheats.

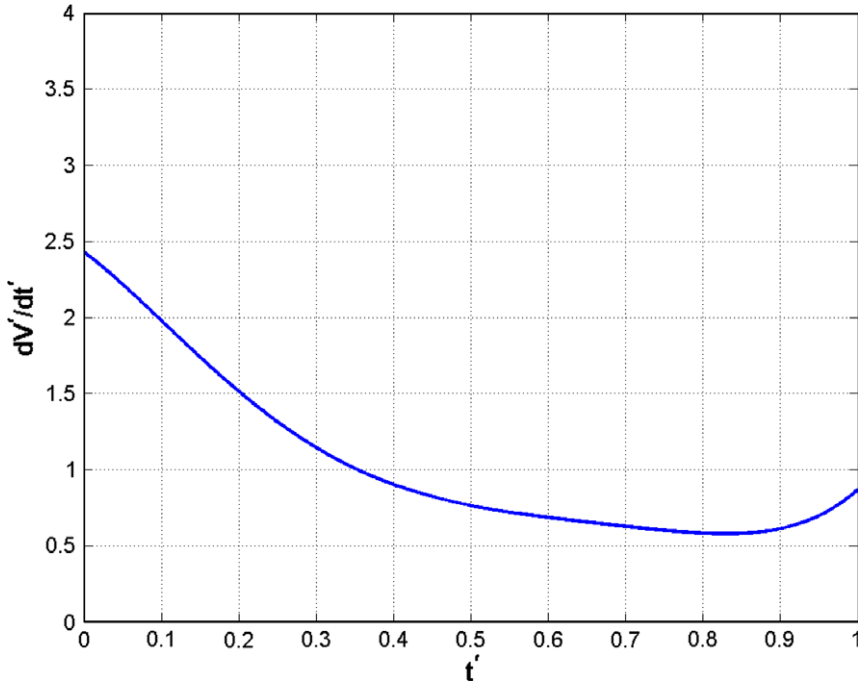

Fig. 6. Vapour production rate.

exhibit oscillations that reflect oscillations of the bubbles during their growth. These oscillations are caused by the preceding bubble at departure: in some situations, the departing bubble touches the new bubble, particularly when the latter is growing too fast. In some other cases, the departing bubble draws the next bubble up when rising in the liquid. The oscillations are more significant when the wall superheat is high: the bubble growth velocity is much higher, so that the new bubble is more likely to reach the previous one and to be influenced by it. Furthermore, since the rising velocity of the previous bubble is independent of the wall superheat while the growth time is decreasing with an increasing superheat, the ratio of bubbles interaction to the total growth time is larger when the superheat is high. These oscillations may have a significant impact on the formation of the thermal boundary layer and on heat transfer during the beginning of the bubble growth. Therefore, this phenomenon should definitely be included in bubble growth models.

Vapour detachment frequency has also been computed (Fig. 8). The frequency is based on the count of departing single bubbles as long as no coalescence occurs, and on the count of departing

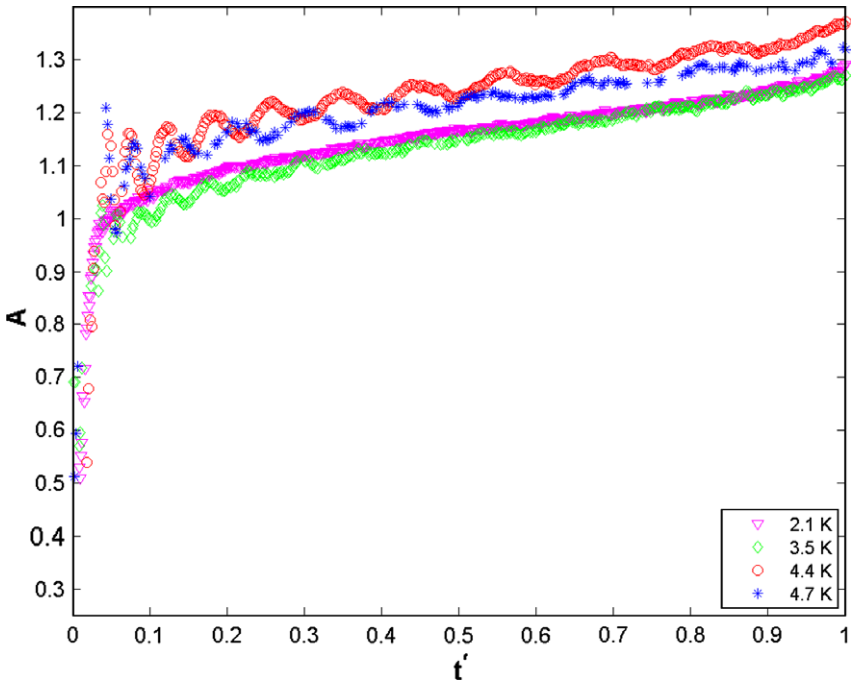

Fig. 7. Height of the centre of gravity divided by the equivalent radius: $A = h_{cg}/R_{eq}$.

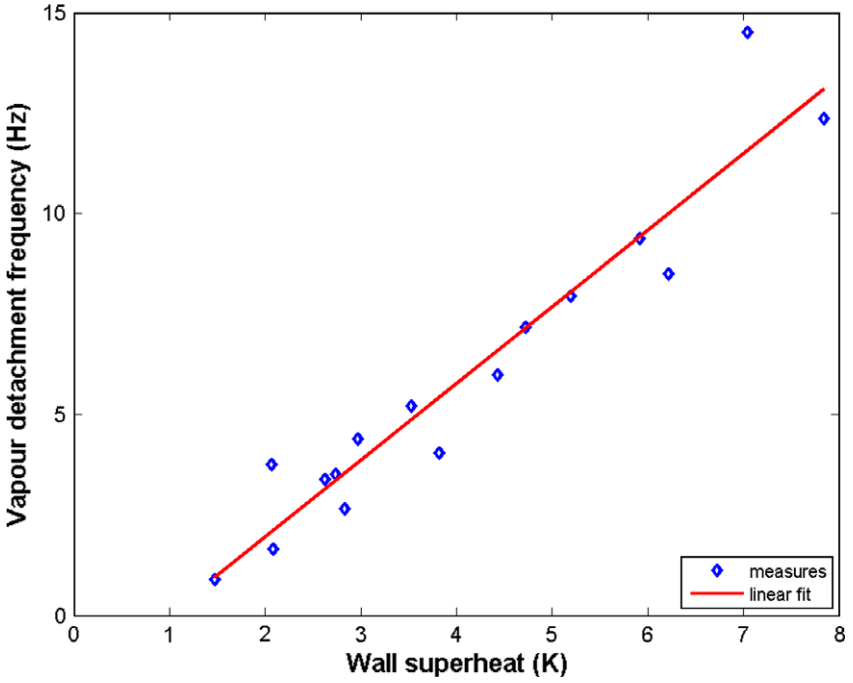

Fig. 8. Vapour detachment frequency.

coalesced bubbles otherwise ($T_{wall} - T_{sat} > 6$ K). The frequency has been computed for 20 consecutive departing bubbles. Coalescence implies a larger dispersion of the frequency values around their mean, since this phenomenon presents a certain random character. At low wall superheat ($T_{wall} - T_{sat} < 2$ K), the nucleation site tends to be deactivated. The frequency increases linearly with the wall superheat. As the bubble detachment volume remains the same, the heat flux increasing mechanism for single bubble boiling when increasing the superheat is the vapour frequency.

Lateral bubble merging has been visualized (Fig. 9) on the double site test sample. Nucleation sites are both active when the wall superheat is between 6.5 K and 9 K. For higher superheats, vertical coalescence occurs, until creating a vapour column. For lower superheats, one of the two nucleation sites gradually becomes deactivated, and the heat flux in the wall is deflected to the site that remains active.

Fig. 9a shows the lateral merging of two bubbles with a wall superheat of 8.5 K. A bubble nucleates at the same time in each nucleation site. Both bubbles grow at the same velocity. Once the bubbles diameter is large enough, both liquid–vapour interfaces are very close, so that there only remains a thin liquid film between the bubbles. Then, the liquid film breaks up, and coalescence

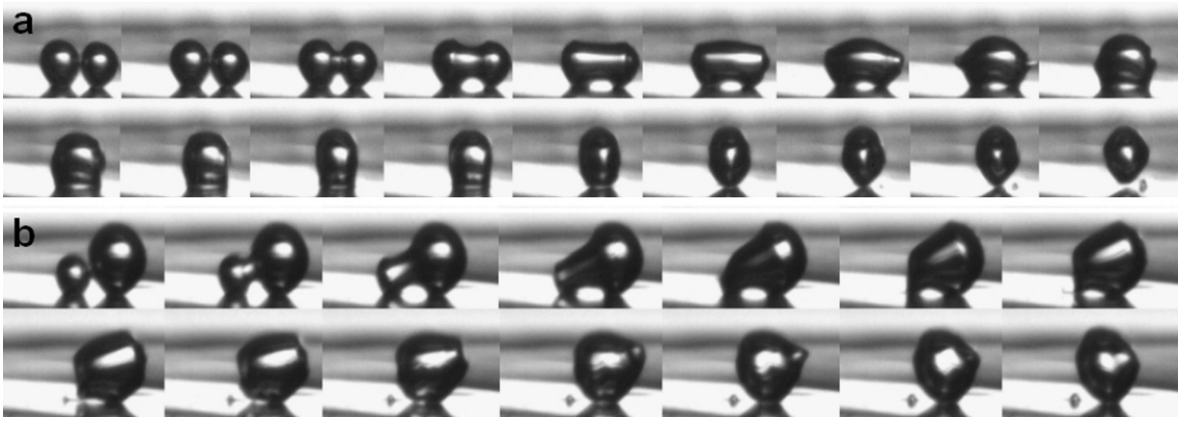

Fig. 9. Lateral bubble coalescence with (a) two bubbles of same size or (b) different size (5400 fps, i.e., 1 image out of 5 at 27,000 fps).

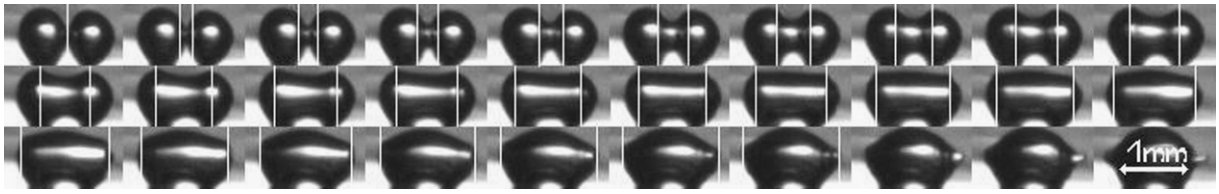

Fig. 10. Wave front propagation during lateral coalescence (27,000 fps, total time: 1.1 ms).

occurs. The circular opening between the bubbles grows fast until the vapour forms a single resulting bubble. The liquid macrolayer volume between the bubbles necks decrease until the macrolayer disappears. Both necks then come free, and the resulting bubble forms a new neck that touches the wall just in between the two preceding necks. Then, the bubble leaves the wall and starts rising in the liquid, and both nucleation sites are almost instantaneously activated again. The coalesced bubble oscillates, and has a bigger inertia than a single non coalesced bubble. Therefore, it accelerates slowly, and often vertical coalescence occurs with the next bubbles.

In our experiments, no influence on the phase change was detected during coalescence: indeed, the vapour production is less than 0.01 mm^3 between the time when the bubbles touch each other (just before the breakage of the liquid layer) and the time when the coalesced bubble departs from the wall while the typical volume of a single bubble at detachment is about 1 mm^3. This is especially due to the quickness of the phenomenon: typically 2–3 ms, whereas the growth time range is 70–300 ms. These results tend to prove that the liquid film between the bubbles does not evaporate, but is rather pushed away by capillary effects. This conclusion is also drawn for the liquid macrolayer trapped between the two necks.

The liquid film breakage induces the propagation of two wave fronts (see Fig. 10 and Electronic Annex 1 in the online version of this article) at a velocity of about 63 cm/s. This front distorts the liquid–vapour interface. When the wave fronts reach the ends of the resulting bubble, tails are created by the distortion of the interface. Such tails have been shown by Mukherjee and Dhir [15]. The wave is then reflected and attenuated. This wave can be explained by capillary effects: the Laplace–Young equilibrium is obtained before the film breakage, and as both main curvature radii are large ($R_1 \approx R_2 > 10^{-4}$ m, same order of magnitude as the bubble equivalent diameter), the pressure difference between the liquid and the vapour is low ($P_{vapour} - P_{liquid} < 3 \times 10^{-3}$ bar). When the film breaks up, its thickness is about 1–10 μm [19]. The smallest curvature radius (R_1) just after the breakage is of the same order of magnitude. The deficit of pressure of the liquid, compared to the Laplace–Young equilibrium, is then of the order of magnitude of 0.1 bar. The shock that creates the wave front on the interface is caused by this deficit of pressure. For a better understanding of the orders of magnitude of R_1 and R_2, Fig. 11 shows schematically half of two bubbles (drawn as two halves of spheres), during the merging process: this schematically shows that R_1 is much smaller than R_2.

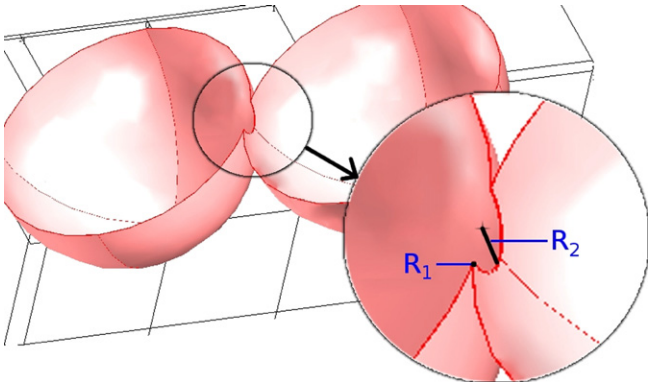

Fig. 11. Interface geometry and main curvature radii after film breakage when merger occurs.

Lateral coalescence has also been observed with two bubbles of different sizes (Fig. 9b). It appears that the smallest bubble is sucked into the biggest one. This phenomenon is due to a higher pressure inside the small bubble than inside the big one.

4. Conclusion

Boiling has been experimentally studied on a single and on two neighbouring nucleation sites. Bubble growth appears very reproducible, the volume at detachment being independent of the wall superheat, whereas the growth time is dependant on the

superheat. Bubble growth rates follow a non-dimensional law as $V' = t'^{0.6}$ for $t' > 0.2$ and $V' = 2 \times t'$ for $t' < 0.2$. This law holds true for any wall superheat in our experiments. These results are very different from those obtained from most analytical models, especially in the sense that the vapour production rate is predicted by these models as increasing during the bubble growth, contrarily to our observations. This shows that much work is still needed in order to describe properly heat and mass transfer during bubble growth.

Oscillations of a growing bubble have been detected and quantified from a dimensionless parameter. This brings to the fore that a departing bubble influences the growth of the following bubble. The interaction is therefore a significant factor that should definitely be taken into account in the models of bubble growth.

The bubble frequency has been found to be approximately proportional to the wall superheat. As the departure diameter is invariant, the product $f \times d$ is also proportional to the wall superheat, and not a constant as it is assumed in many models.

Bubble coalescence between two neighbouring bubbles has also been studied. The results tend to show that coalescence does not have a great impact on vapour production during merging, and that the macrolayer between the bubbles is removed because of capillary effects rather than because of its vaporization. The presence of strong capillary effects has been emphasized by the observation of a wave front propagation.

Acknowledgment

This work was prepared in the frame of the CNRS thematic network GDR3057 "Analyse, Maîtrise des Ecoulements et Echanges Thermiques", AMETh.

Appendix A. Supplementary material

Supplementary data associated with this article can be found, in the online version, at doi:10.1016/j.expthermflusci.2008.04.004.

References

[1] I. Golobic, J. Petkovsek, M. Baselj, A. Papez, D.B.R. Kenning, Experimental determination of transient wall temperature distributions close to growing vapor bubbles, in: ECI International Conference on Boiling Heat Transfer, Spoleto, 2006.
[2] D.C. Cheng, H. Burkhardt, Template-based bubble identification and tracking in image sequences, International Journal of Thermal Sciences 45 (2006) 321–330.
[3] C.W.M. Van der Geld, Prediction of dynamic contact angle histories of a bubble growing at a wall, International Journal of Heat and Fluid Flow 25 (2004) 78–80.
[4] P. Di Marco, W. Grassi, G. Memoli, Experimental study on rising velocity of nitrogen bubbles in FC-72, International Journal of Thermal Sciences 42 (2003) 435–446.
[5] A. Vasquez, R.M. Sanchez, E. Salinas-Rodriguez, A. Soria, R. Manasseh, A look at three measurement techniques for bubble size determination, Experimental Thermal and Fluid Science 30 (2005) 49–57.
[6] N. Zuber, The dynamics of vapor bubbles in nonuniform temperature fields, International Journal of Heat and Mass Transfer 2 (1961) 83–98.
[7] M.S. Plesset, S.A. Zwick, The growth of vapor bubbles in superheated liquids, Journal of Applied Physics 25 (1954) 493–500.
[8] L.E. Scriven, On the dynamics of phase growth, Chemical Engineering Science 10 (1959) 1–13.
[9] B.B. Mikic, W.M. Rohsenow, P. Griffith, On bubble growth rates, International Journal of Heat and Mass Transfer 13 (1970) 657–666.
[10] M.G. Cooper, A.J.P. Lloyd, The microlayer in nucleate pool boiling, International Journal of Heat and Mass Transfer 12 (1969) 915–933.
[11] A.K. Das, P.K. Das, P. Saha, Heat transfer during pool boiling based on evaporation from micro and macrolayer, International Journal of Heat and Mass Transfer 49 (2006) 3487–3499.
[12] G. Hetsroni, A. Mosyak, E. Pogrebnyak, I. Sher, Z. Segal, Bubble growth in saturated pool boiling in water and surfactant solution, International Journal of Multiphase Flow 32 (2006) 159–182.
[13] Z. Yin, A. Prosperetti, J. Kim, Bubble growth on an impulsively powered microheater, International Journal of Heat and Mass Transfer 47 (2004) 1053–1067.
[14] J. Bonjour, M. Clausse, M. Lallemand, Experimental study of the coalescence phenomenon during nucleate pool boiling, Experimental Thermal and Fluid Science 20 (2000) 180–187.
[15] A. Mukherjee, V.K. Dhir, Study of lateral merger of vapor bubbles during nucleate pool boiling, ASME Journal of Heat Transfer 126 (2004) 1023–1039.
[16] L. Zhang, M. Shoji, Nucleation site interaction in pool boiling on the artificial surface, International Journal of Heat and Mass Transfer 46 (2003) 513–522.
[17] M. Barthès, Boiling on a single nucleation site: experimental study of the bubble growth dynamics and of the associated heat transfers, Ph.D. thesis (in French), Université de Provence, 2005, p. 161.
[18] H.C. Lee, B.D. Oh, S.W. Bae, M.H. Kim, Single bubble growth in saturated pool boiling on a constant wall temperature surface, International Journal of Multiphase Flow 29 (2003) 1857–1874.
[19] S.T. Revankar, Coalescence and breakup of fluid particles in multi-phase flow, 4th International Conference on Multiphase Flow, New Orleans, 2001, paper 352.